3 Absolute Configuration and Conformational Analysis of Chiral Compounds via Experimental and Theoretical Chiroptical Methods: ORD, ECD, and VCD

A.G. Petrovic, N. Berova, J.L. Alonso-Gómez

Methodology, scope and advantages of ECD, VCD and ORD are presented in a **tutorial way** to help in choosing a suitable combination of spectroscopic tools when facing a quest for structural elucidation for small-medium organic chiral molecules.

3.1 Chirality

The Gold Book of the IUPC defines chirality as "*The geometric property of a rigid object (or spatial arrangement of points or atoms) of being non-superposable on its mirror image; such an object has no symmetry… a mirror plane, a center of inversion, a rotation-reflection axis. If the object is superposable on its mirror image the object is described as being achiral.*" Even dating back to 1904, Lord Kelvin stated in his Baltimore Lectures on Molecular Dynamics and the Wave theory of Light: "*I call any geometrical figure, or group of points, chiral, and say that it has chirality if its image in a plane mirror, ideally realized, cannot be brought to coincide with itself.*" The phenomenon of chirality is also found on molecular scale, when molecular architectures incorporate chiral elements such as chirality axis, chirality center or chirality plane (Figure 3. 1).

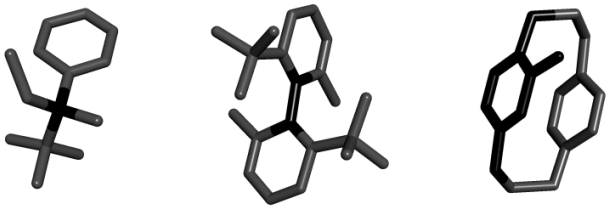

Figure 3. 1 Representation of molecules incorporating different chirality elements in black from left to right: chirality center, chirality axis and, chirality plane.

Chiral molecules exhibit enantiomerism, a form of isomerism that consists of two molecular entities, called enantiomers, which are non-superimposable mirror-image forms of each other. The behavior of two enantiomers is indistinguishable when they interact with an achiral entity. However, they may interact differently with a chiral entity (either another chiral molecule or chiral light). As an example, thalidomide was used as a racemate (50:50 mixture of the two enantiomers) in the late 50s and early 60s to treat morning sickness in pregnant women. While the (*R*)-thalidomide is an efficient sedative, its enantiomer, designated as (*S*)-thalidomide, resulted in birth defects in thousands on newborns.[1] The different physiological response of these two enantiomers

can be explained by the fact that mechanism of action for most drugs involves interaction with chiral proteins present in the body. In a similar way, the two enantiomers may behave differently when interacting with a chiral electromagnetic wave since they induce diastereomeric interactions. From this phenomenon emerges chiroptical spectroscopy.

3.2 What is a chiroptical method?

Enantiomeric and diastereomeric forms of chiral molecules may respond differently when interacting with light. This phenomenon is often used for the absolute configuration (AC) and conformational analysis assignments. Electromagnetic radiation is composed of perpendicular electric and magnetic in-phase periodic fields, both oscillating in a plane perpendicular to the light propagation. Linearly polarized light (LPL) presents a plane of electric field oscillating along a straight line (Figure 3. 2a). A new electric filed merges following the rules of vector addition when two electric fields are superposed. As an example, when two perpendicular linearly polarized electric fields are superposed with the same, wavelength, phase, and amplitude, a new plane polarized wave arises at 45º (Figure 3. 2b). However, ±90º phase difference between the two perpendicular waves results in a right or left circularly polarized forms of light, which are enantiomeric to each other (Figure 3. 2c and Figure 3. 2d). Interestingly, the superposition of two circularly polarized lights (CPL) of opposite twist but same wavelength, phase and, intensity results in a linearly polarized wave (Figure 3. 2e).

Spectroscopy exploits the interaction between electromagnetic waves and matter with the aim for structural elucidation. When a linearly or circularly polarized light travels across an absorbing medium its amplitude decreases since part of its intensity is used to induce excitations within the molecular framework of the matter (Figure 3. 2f and Figure 3. 2g). Depending on the energy range of the light source, a chiral compound may absorb differently right and left circularly polarized light, in which case the phenomenon presents circular dichroism (CD). As mentioned above, a linearly polarized light can be represented as the superposition of a left and a right CPL. In a matter exhibiting circular dichroism where right CPL is not absorbed and left CPL is partially absorbed, an initial LPL will be transformed into an elliptically polarized light (Figure 3. 2h). In a matter exhibiting refracting index greater than one, the light slows down and as a consequence a different phase is observed between the wave before and after crossing it (compare Figure 3. 2a with Figure 3. 2i for LPL and Figure 3. 2c with Figure 3. 2j for CPL). A chiral matter may present birefringence when the refractive index for left and right CPL is different. Once linearly polarized wave travels across a birefringence matter, the two CPL components travel at a different speed causing a

polarization-plane rotation of the LPL (Figure 3. 2k). Most commonly, a chiral matter exhibits both circular dichroism and birefringence, and therefore a linearly polarized light is transformed into an elliptically polarized light where the long axis has been rotated with respect to the polarization of the incident LPL (Figure 3. 2l).

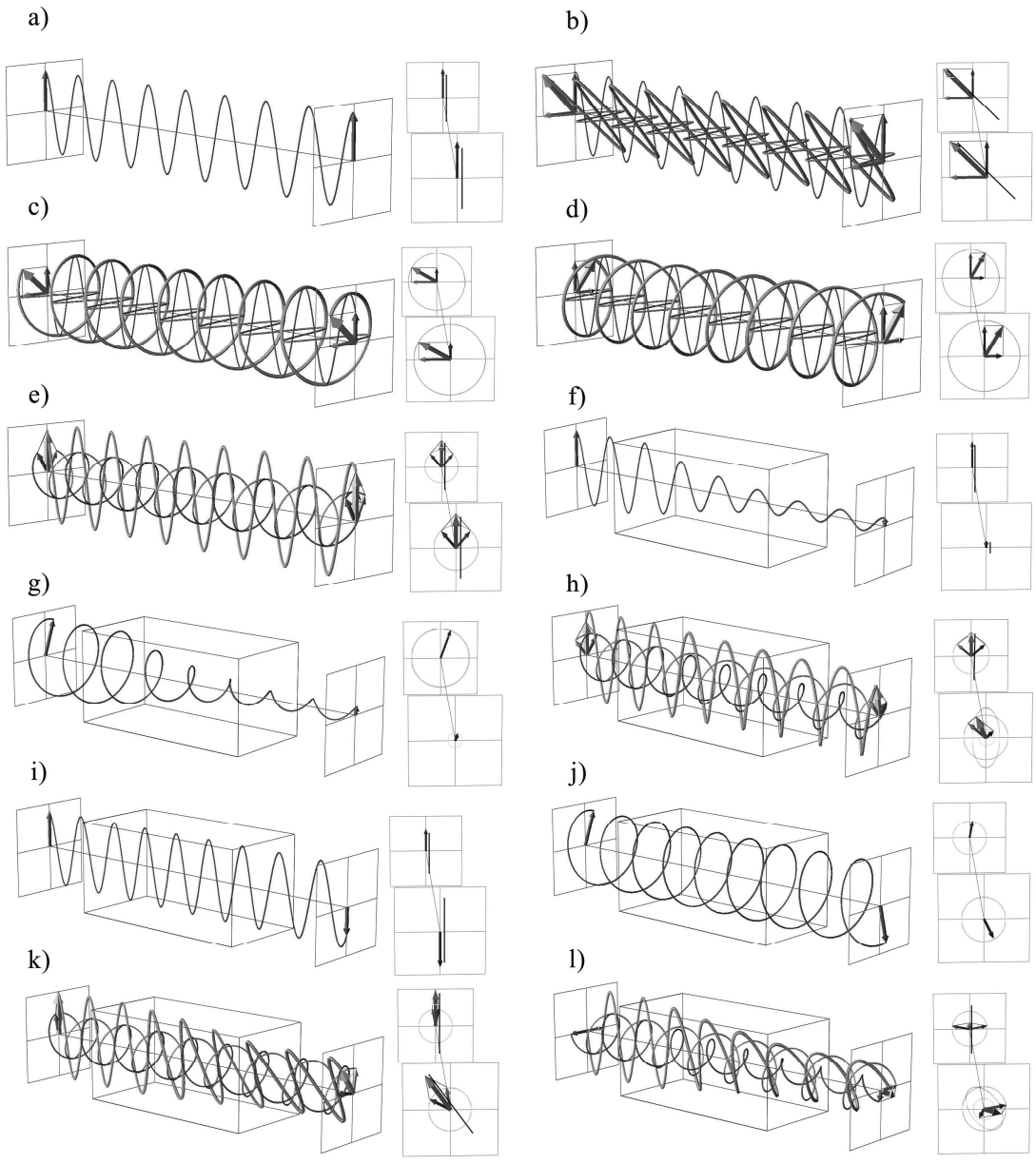

Figure 3. 2 Representation of the wave propagation in space. The vectors represent the direction and intensity of the field measured at a particular location. For the sake of clarity, projections on planes perpendicular to the trajectory are sketched for the starting and ending points of every trajectory.

For a chiral sample, the optical rotation $[\alpha]$ and the circular dichroism $\Delta\varepsilon$ at a particular wavelength can be extracted from the experimental elliptically polarized light (Figure 3. 3).

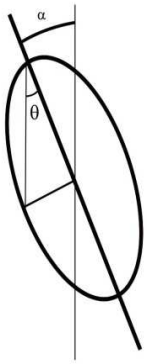

Figure 3. 3 Representation of the elliptically polarized light with optical rotation.

For small angles, the ratio of the minor *vs.* the major axis of the ellipse is equal to $\tan\theta$ and is referred to as ellipticity. This observable, typically recorded in mdeg units is a consequence of the $\theta = 32.98\,\Delta A$, where ΔA is the difference between the abortion of the right and left CPL. Ellipticity can be easily transformed into molar ellipticity $[\theta] = \frac{100\theta}{Cl}$, where C is the concentration in molL^{-1} and l is path length in cm^{-1}. Now, the molar circular dichroism can be expressed like $\Delta\varepsilon = \frac{[\theta]}{3298}$. On the other hand, specific rotation is typically defined as $[\alpha] = \frac{100\alpha}{c_p l}$, where α is the angle between the incident plane of polarization of light and the long axis of the elliptically polarized light, c_p in the concentration in 100 g cm^{-3}, and l is the path length in dm.

Molecules interact with electromagnetic fields by absorbing energies coinciding with the gap between ground and excited states. When the electromagnetic field is in the ultraviolet visible (UV/Vis) energy range, electronic transitions may occur. Similarly, electromagnetic fields in the infrared (IR) region induce different vibrational transitions. The chiroptical methods exploit different ranges of the spectra (Figure 3. 4).

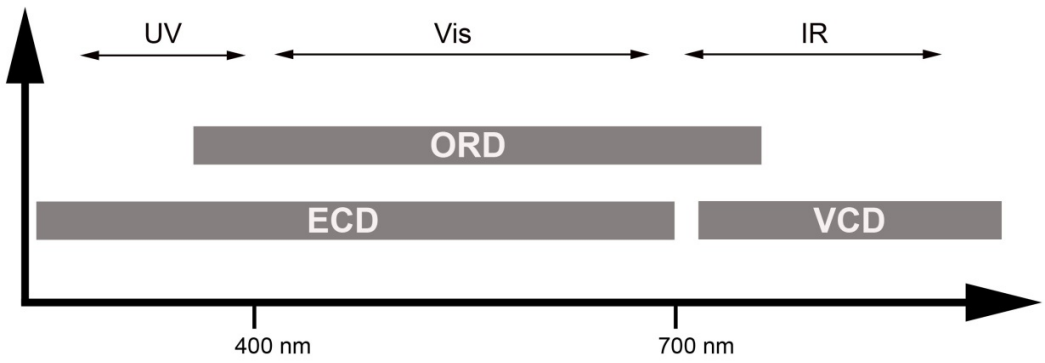

Figure 3. 4 Representation of the energy ranges by different chiroptical methods.

The energy of a band in the UV/Vis spectra directly depends on the energy gap between the ground and a particular excited electronic state, while the intensity is provided by the dipole strength $D = \vec{\mu}^2$, where $\vec{\mu}$ is the electric transition dipole moment (ETDM). Since ETDM is like a state function, as it depends only on the electron density´s initial and final states, it is identical for pairs of enantiomers. However, the intensity and sign of a band appearing in the CD spectra is proportional to the rotatory strength $R \sim \vec{\mu} \cdot \vec{m} = |\mu||m| \cos\beta$, where $\vec{m}$ is the magnetic transition dipole moment (MTDM) and β the angle between the electric and magnetic transition dipole moments. The MTDM is the magnetic moment generated due to the displacement of electron density during the transition. Both $|\mu|$ and $|m|$ are the same for a pair of enantiomers, yet the angle between them is different (Figure 3. 5). The sign of the dichroic band will be positive if $\beta < 90°$ and negative if $\beta > 90°$. The rotatory strength has the same magnitude but opposite sign for a particular transition in a pair of enantiomers and, as a consequence, their CD spectra are mirror image of each other.

A chiroptical property which is also related to the rotatory strength is optical rotatory dispersion (ORD), a rotation of LPL when interacting with a chiral molecule at different wavelengths (λ). Quantum mechanics (*ab initio*) is able to predict the energy as well as the D and R of electronic transitions and, therefore, the UV/Vis and CD spectra of any chiral molecule can be simulated (Figure 3. 5). Programs like Gaussian 09 give the optical rotation for the required λ. Similarly, the IR and vibrational circular dichroism spectra (VCD) can also be theoretically predicted.

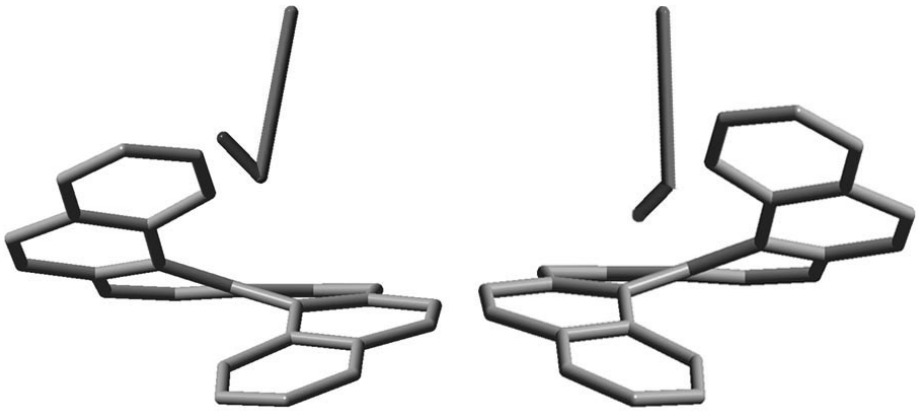

*Figure 3. 5 ETDM (short bars) and MTDM (long bars) representation for the lowest electronic transition of (*P*)-[7]helicene, left and (*M*)-[7]helicene, right. Simulated with ZINDO.*

For the construction of the final chiroptical spectra, dipole and rotational strengths for each of the normal modes need to be converted to molar extinction coefficients. The simulation of the UV/Vis spectra can be easily carried-out using the equation:

$$\varepsilon(\nu) = \frac{D_i \nu_i}{4 * 2.296 \times 10^{-39} \sqrt{\pi}\sigma} \exp\left[-\left(\frac{\nu - \nu_i}{\sigma} \right)^2 \right]$$

where σ is the band-with in eV, taken as the mid-height width (typically $\sigma \approx$ 0.2–0.4 eV), while frequencies ν are in cm^{-1}.[2] Similarly, the ECD spectra can be obtained using the following equation:

$$\Delta\varepsilon(\nu) = \frac{R_i \nu_i}{2.296 \times 10^{-39} \sqrt{\pi}\sigma} \exp\left[-\left(\frac{\nu - \nu_i}{\sigma} \right)^2 \right]$$

Chiroptical spectroscopies are dependent not only on the configuration but also on the conformation of the molecules and therefore the comparison of theoretically predicted and experimental ECD, ORD and VCD are often used for the overall structural characterization of chiral molecules. As a consequence of the chiroptical response dependence on the overall geometry of the system, establishment of the potential energy surface (PES) is necessary before the spectral simulation.

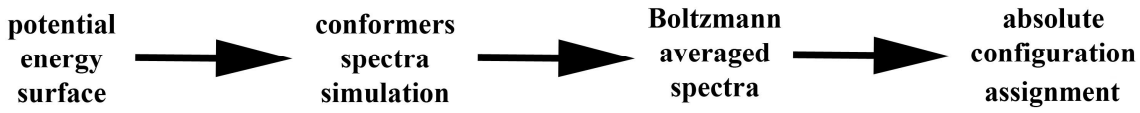

Figure 3. 6 General procedure to determine de AC of a molecule with the combination of experimental and theoretically predicted chiroptical responses.

Generally, four steps should be followed to determine the AC of an organic molecule (Figure 3. 6). After the PES has been surveyed, the spectra for all stable conformers significantly present in solution (typically with energy not higher than 3 kcal mol^{-1} above the global minimum) should be simulated. Subsequently, one needs to generate average spectra considering the relative population of the conformers as determined by the Boltzmann equation. Finally, the comparison of the averaged spectrum and the experimental one may yield the AC assignment (see Chapter 2 for a more detail explanation). Within a domain of VCD spectroscopy there is an increasing compliance to a quantitative level of comparison, while within domains of ECD and ORD spectroscopies, the comparison is mostly qualitative.

3.3 Quantum Mechanical (*ab initio*) methods for predicting chiroptical properties:

The theoretical prediction of chiroptical properties has become one of the streamline applications of quantum chemistry in the last two decades. The most renowned program package that provides *ab initio* tool-box for predicting the chiroptical responses is Gaussian,[3] with lastly implemented G09 version. Even though computer programs such as Gaussian are available nowadays for nearly automated use as "black-box" applications, in order to avoid inaccurate chiroptical predictions and wrong conformational interpretations along with stereochemical assignments, users have to become aware of the scope of computational methods under consideration. The reliable determination of the AC requires optimal choice of the computational method, also referred to as the level of theory: i.e. HF, MP2, DFT along with the selection of functionals and basis sets. For predicting electronic chiroptical properties, ORD and ECD, the most conferred quantum mechanical approaches are DFT and coupled-cluster (CC) theory.[4]

The highly correlated wave-function based methods like CC and Complete Active Space Self-Consistent Field (CASSCF) methods have been reported to be more accurate than any DFT functional. However, the challenge with such predictions is that they are substantially time-consuming and are restricted to smaller molecules. The more cost-effective method of choice has hence been DFT. Even though the initial DFT-based calculations of ORD were not accurate near the resonance frequencies (region were electronic transitions occur), the improved implementation of the DFT method has overcome this limitation.[5] Furthermore, as it will be emphasized in section

3.6, when predicting optical rotation, it is essential to calculate this property at several wavelengths especially when the theoretically predicted and/or experimentally obtained response at a given wavelength is less than ±100° This rule holds true regardless of the choice of *ab initio* method for optical rotation prediction.

Similarly to the discussion associated with ECD and ORD, higher electron-correlation methods like MP2, are computationally too demanding and hence are currently not suggested for predicting VCD. By now, it is generally accepted that DFT theory applied for VCD consideration yields more accurate results than the electron-correlation deprived HF approach. Wide adoption of DFT since the 1990s had brought its dominance in predicting chiroptical properties as it provides reasonably accurate results at moderate computational cost.

The DFT theory mandates the selection of density functionals and basis sets. Hybrid functionals B3LYP and B3PW91 are most frequently used as they give the best agreement with experimental observations while simpler functionals yield less accurate results even when combined with relatively large basis sets.[6] Nonetheless, the so called CAM-B3LYP functional has been shown to provide a more optimal reproduction of both the position and the intensity of the experimental ECD peaks in comparison to generally more popular hybrid B3LYP functional.[7][8] It is worth noting additionally that recent chirality studies have alluded to the use of a newer generation DFT functional, so called M06-2X, which has been reported[9] to provide good accuracy in reproducing relatively stabilities of conformers in solution.

In terms of the basis sets, the current consensus is that the smallest level basis set recommended for chiroptical predictions is 6-31G* (also referred to as 6-31G(d)). In some cases, dramatic quantitative improvements have been noted by increasing the size of the basis set to TZ2P and cc-pVTZ.[10] Both polarization and diffuse basis sets such as 6-311++G**, cc-pVDZ, cc-pVTZ are necessary to predict the important experimental VCD features for molecules with propensity for intra- or inter-molecular interactions. Also, in particular cases, the reliable ECD and ORD predictions require the use of moderate to large basis sets (i.e. 6-311++G**, cc-pVDZ, cc-pVTZ).[11]

The intensity and occasionally even the sign of chiroptical responses are sensitive to the molecular environment. The chiroptical response perturbations induced by solute-solvent interactions translate into the need for *ab initio* solvent consideration in cases where such interactions are anticipated. If specific directional solute-solvent interaction is known, then spectral effect should be considered with an explicit solvent model.[12]

As an example, in VCD spectroscopy, the shift of experimental vibrational absorption (VA) bands can provide insight into intermolecular interactions (i.e. H-bonding typically results in the lower frequency stretching modes due to borrowed electron density). When employing an explicit

solvent model, prior to subjecting the chiral solute-solvent system to the geometry optimization, one should apply either Monte Carlo or Molecular Dynamics algorithms to determine the optimal initial orientation(s) of the explicit solvent relative to the chiral solute. Less rigorous prediction which also accounts for solvent effect implicitly involves the use of polarizable continuum solvent models (IEF-PCM being the most popular) or conductor-like screening solvent models (CPCM, COSMO).[10] It is worth noting that recently there have been suggestions that in order to achieve a more efficient geometry optimization of the system which includes an explicit solvent model, one should simultaneously apply the corresponding implicit solvent model. The sole implementation of the implicit solvent models is suitable for case studies where intermolecular interactions, such as Van der Waals, are anticipated, but the exact directionality of these interactions is more ambiguous.

With respect to the calculated vibrational frequencies, in VCD spectroscopy these are usually overestimated and hence should be downscaled by a constant which is dependent on the specific basis set used. The effect that causes non-uniform shifts in predicted VA and VCD band positions relative to the observed ones is attributed to vibrational anharmonicity. Similarly, scaling and/or shifting of the predicted ORD or ECD are generally accepted to provide a better resemblance with the experimental data. The future improvements of the application of *ab initio* methods will need to account for these effects. Nevertheless, rapid improvements within quantum theory models as well as computational power capacities are paving the way for elucidating the structure of increasingly more chemically complex chiral systems.

3.4 Electronic Circular Dichroism (ECD)

ECD is the most used chiroptical method to date. Firstly, it has been used with empirical correlations rules such as the octant rule. However, the application of this method is limited by the need for particular prerequisites in the structure of the studied chiral system. On the other hand, the exciton chirality method has been successfully applied in a large number of cases. This method, nevertheless, needs the presence of two appropriate chromophores in a molecule. Thanks to the fast development of *ab initio* methods, nowadays ECD combined with theoretical simulations is used in the stereochemical elucidation of a broad variety of compounds.

It is worth mentioning that even though majority of *ab initio* based ECD studies are complemented by solution state experimental measurements, in more recent years there have been reports of solid state ECD studies.[13] The key reported advantage of employing a solid state ECD is that by knowing the solid-state geometry (X-ray structure), one may use it as

the input structure for *ab initio* ECD calculations and hence bypass the challenges associated with the conformational flexibility in a solution state. Nonetheless, great care should be taken in avoiding artifacts due to linear birefringence effects.

3.4.1 Advantages of ECD

- Very small amount of compound is needed due to its high sensitivity (of about 10^{-5} M solutions are required).
- Very easy to measure. The same sample can be used for UV/Vis measurement.
- Availability of ECD spectrometers.
- When suitable chromophores are present the AC can be easily assigned by exciton chirality.

3.4.2 Limitations of ECD

- The molecule should bare chromophores, the presence of an UV/Vis band is necessary to enable an ECD band in a particular region of the spectrum.
- Moderate to low signal resolution, therefore only few different bands are present in the spectra.
- The theoretical prediction of the spectra needs the prediction of electronic excited states.
- The presence of significant vibronic coupling may be difficult for the analysis.

3.4.3. Applications of ECD

The text below describes several methods that have been developed over the years as means of establishing the AC assignment of chiral molecules as tackled by ECD spectroscopy.

3.4.3.1. Empirical methods

The presence of dichroic bands in the ECD spectrum of an isotropic media is empirical evidence for the existence of chiral systems. In this way, simply the presence of ECD signals has been proven to be very efficient in the relative configuration assignment. As an example, the synthesis of allenophanes was carried out starting form racemic allenes providing a diastereoisomeric mixture. Even though Nuclear Magnetic Resonance (NMR) techniques helped in the assignment of some of the diastereoisomers, they could not discriminate between few isomers with very similar symmetry. The ECD analysis of different fractions resolved via HPLC using a chiral stationary phase (CSP) was crucial to discriminate between chiral and achiral stereoisomers. The enantimeric isomers present mirror image spectra while the achiral isomers do not show any signal in the ECD.[4, 5]

The best known empirical chirality rule has been used for the characterization of saturated ketones and aldehydes. These intrinsically achiral chromophores show a $n \longrightarrow \pi^*$ transition in the UV region (~300 nm). In the so called octant rule, the carbonyl group is placed in the center of three nodal planes dividing eight sectors. Any atom or group of atoms located at a particular sector will contribute to the CD signal with a positive or negative term defined by the particular sector. The summation of all contributions will give the estimated CD band (Figure 3. 7).

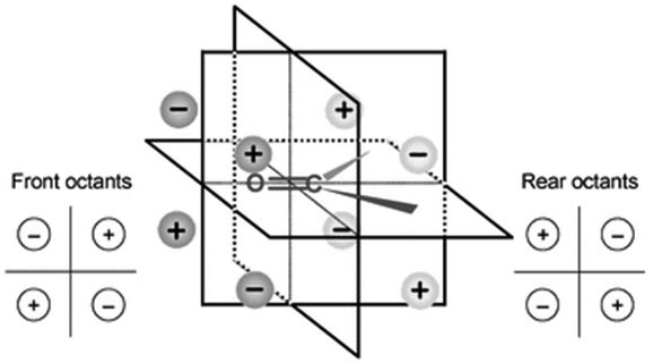

Figure 3. 7 The nodal planes of the chromophore define 8 octants; the signs of the contributions to the CD of the band around 300 nm are shown.[14]

However, when more than one group is located in oppositely signed octants, it may not be clear which has the larger contribution. Additional challenge associated with this empirical method is that the presence of more than one conformer may decrease the reliability of configurational assignment.[14]

3.4.3.2. Exciton coupling

When measuring UV/Vis or ECD spectra of a solution, typically concentrations are below 10^{-4} molL^{-1}. Under these conditions the average intermolecular distance is longer than 10 nm, and therefore interaction between two molecules are neglected when considering compounds having $\varepsilon = 10^4$ L mol^{-1}cm^{-1}. The question to consider next is: what happens when two chromophores are placed in the same molecule? In a molecule bearing two identical chromophores fixed in the space with no conjugation between them, both chromophores have the same probability to undergo an electronic transition. However, in presence of exciton coupling, the otherwise degenerated transitions split into two excited states, which is phenomenon referred to as Davydov splitting.

As mentioned above, the electric transition dipole moment $\vec{\mu}$ is that vector that indicates the orientation in which the electron density is displaced upon excitation. However, when a chromophore is excited, both orientations along $\vec{\mu}$ are equally probable for the electron

displacement. Consequently, when two chromophores are very close to each other, in-phase and out-of-phase transitions must be considered. In this case, three situations are possible considering the angle θ between them (Figure 3. 8):[15]

- When $\theta = 90°$, in-phase and out-of-phase excitations are equivalent and therefore the observed λ_{max} coincide with the energy absorption of the single chromophore λ_o.
- When $\theta < 90°$, in-phase excitation is energetically less favorable than for the single chromophore, since partial charges of the same sign are close to each other, while the opposite is true for the out-of-phase excitation. The in-phase $\vec{\mu}$ is larger than the out-of-phase $\vec{\mu}$ and therefore $\lambda_{max} < \lambda_o$.
- When $\theta > 90°$, out-of-phase excitation is energetically less favorable than for the single chromophore, since partial charges of the same sign are close to each other, while the opposite is true for the in-phase excitation. The in-phase $\vec{\mu}$ is larger than the out-of-phase $\vec{\mu}$ and therefore $\lambda_{max} > \lambda_o$.

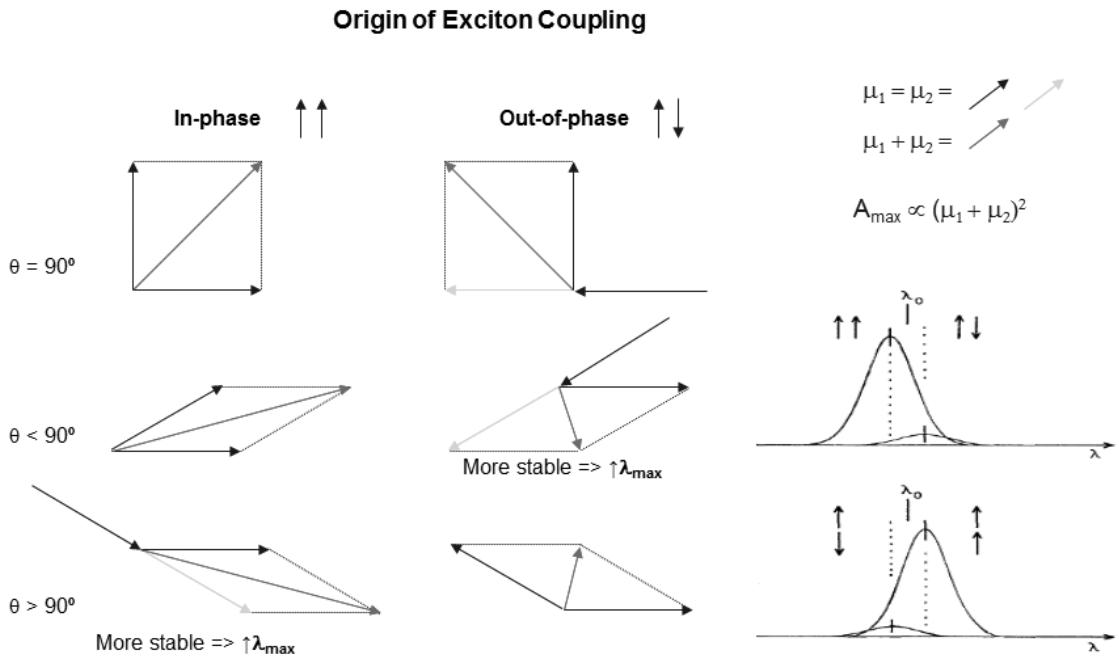

Figure 3. 8 Representation of the possible situations considering the angle θ between $\vec{\mu}$ of two chromophores present in a molecule.

This phenomenon also has consequences on the CD response and it is referred to as exciton chirality. Experimentally a bisignated CD band is observed. When the less energetic band is negative

followed by a more energetic positive one, it is referred to as a negative CD couplet and *vice versa*. As a non-empirical rule,[8] when looking through the center of both chromophores, if the shortest way from the front to the rear chromophore is counterclockwise, it is defined as negative sign and it always presents a negative CD couplet (Figure 3. 9). The opposite is true for a positive CD coupled. As an example, the absolute configuration of allene (*M*)-**1** was unambiguously assigned after derivatization with appropriate chromophores.[16]

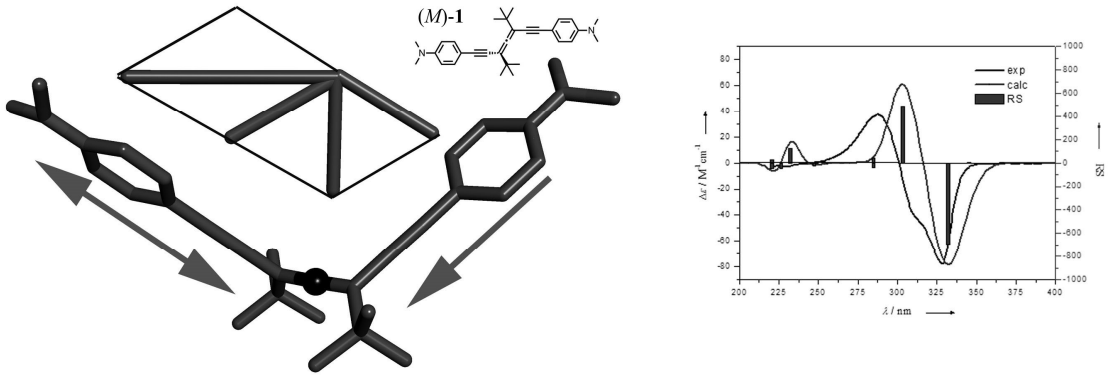

Figure 3. 9 left: Equilibrium geometry of (*M*)-**1** *at the B3LYP/6-31G(d) level of theory. Bars and arrows represent the* $\vec{\mu}$ *for each aniline chromophore as well as the in-phase and out-of-phase total* $\vec{\mu}$*. right: ECD spectrum of* (M)-**2** *(e.r.* ≥ *91:9) recorded in hexane (black line), calculated ECD curve for (M)-2 at the TDDFT B3LYP/6-31G(d) level of theory (s=0.08, scaled to 0.5, gray line), and rotational strengths for the different transitions (gray bars).*[17]

The exciton chirality has been extensively used for the relative and absolute configuration determination of very complex molecules derivatized with benzoates, functioning as the interacting chromophores. Several examples are presented in Chapter 11.

3.4.3.3. ECD simulation via *ab initio* methods: AC and conformation determination

As mentioned above, the interpretation of an ECD spectrum can be trivial occasionally. However, for most of the cases, this interpretation needs the assistance of *ab initio* calculations. Since the chiroptical properties can be predicted theoretically, the comparison of experimental and theoretical responses is a very powerful tool for the AC and conformational determination.

Chiroptical responses, in general, are very sensitive to the geometry of the molecules. Therefore, it is crucial to establish the pool of possible conformers prior to the chiroptical response simulation. The simplest situation is when only one conformer is possible. As an example, the ECD of the allenic compound (*M*)-**1** presented above showing exciton coupling has also been predicted at the TDDFT B3LYP/6-31G(d) level of theory. As shown in Figure 3. 9, the exciton

coupling centered at ~315 nm is very well resembled by the theoretical simulations, therefore, further confirming the AC determined by the exciton chirality method.[17]

Expectedly, the ECD based analysis is more complex when the molecule is more flexible and consequently exhibits multiple stable conformers. An example of such case-study is investigation of thiazolopyrimidine (±)-**2**, which was synthetized as a racemic mixture and the two enantiomers were resolved using HPLC on a chiral stationary phase.[18] In order to determine the AC of both enantiomers, ECD was measured showing two clear Cotton effects at 380 nm and 280 nm (Figure 3. 10). Exploration of the potential energy surface (PES) by manual rotation of torsion angles followed by optimization and frequency calculations at the B3LYP/6-31G(d), afforded five conformers (*R*)-**2a–e** in an energy range of 0.2 kcalmol^{-1} (Figure 3. 11). Since all conformers are very close in energy, upon applying Boltzmann equation, it was found that they are all significantly present in solution.

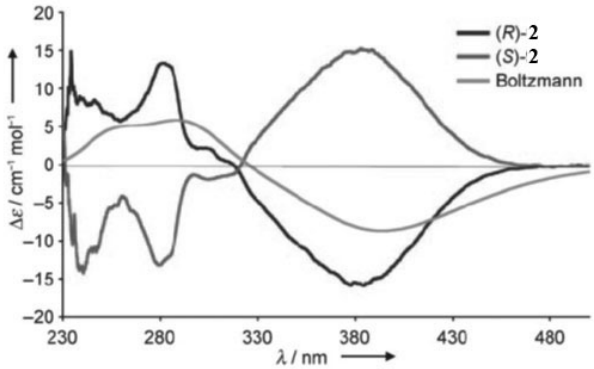

Figure 3. 10 ECD spectra. Experimental spectra in $CHCl_3$ and Boltzmann-weighted ECD simulation for (*R*)-**2** *at the TD-B3LYP/6-31G(d) level of theory.*[18]

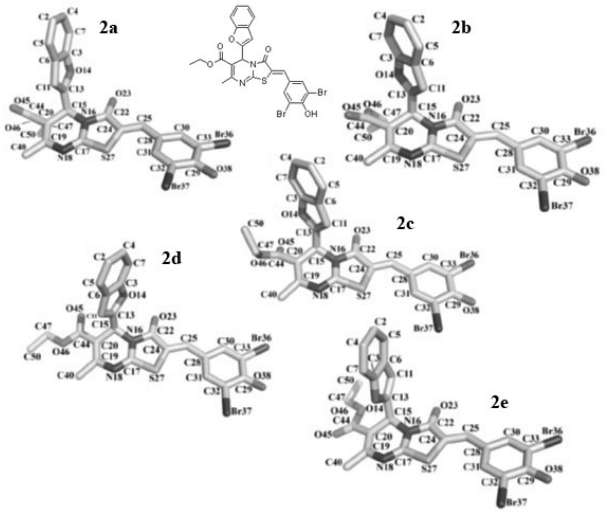

*Figure 3. 11 Conformers (*R*)-**2a**–(R)-**2e**. Scanning of the potential energy surface by systematic variation of torsion angles C15-C20-C44-C45 and N16-C15-C13-O14.*[18]

Accordingly, the ECD spectra for conformers (*R*)-**2a–e** were predicted at the (TD)-B3LYP/6-31G(d) and the Boltzmann-weighted theoretical spectrum was compared with the experimental one. As depicted in Figure 3. 11, the predicted ECD spectra (*R*)-**2a–e** resembles very well the experimental ECD for one of the resolved enantiomers, and therefore the AC could be assigned unambiguously.

As chiroptical responses are very sensitive to the conformation, this phenomenon is often used to determine the conformation of chiral molecules in solution. The reaction of tetracyanoethene with electron reach acetylenes is a very efficient reaction leading to tetracyanobutadienes (TCBDs). In this respect, reaction of the above mentioned (*M*)-**1** with TCNE yielded bis-TCBD (*M*)-**3** (Figure 3. 12).[17]

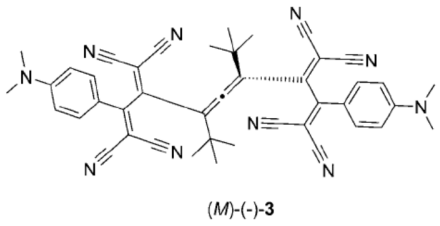

*Figure 3. 12 Structure of bis-TCBD (*M*)-**3**.*[17]

The experimental ECD spectrum exhibits a remarkable Cotton effect at 530 nm. Since electronic transitions around this energy are assigned to charge transfer from the aniline moieties into the TCBDs, this chiroptical response suggests a chiral induction from the allene to the neighboring TCBDs.[17] In order to verify this assumption, the simulation of the ECD spectra was performed.

Manual scan was undertaken to characterize the PES of (*M*)-**3** with systematic torsion angle modifications every 60º for the TCBD moieties. A total of 18 initial geometries were optimized at the B3LYP/6-31G(d) level of theory leading to 15 different conformers, (*M*)-**3a**-**3o**, characterized as true minima by the frequency calculations at the same level of theory. However, the global minimum (*M*)-**3b** is 3.9 kcalmol^{-1} more stable than the second less stable conformer, and, therefore, it is expected that (*M*)-**3b** is the only conformer significantly present in solution. In this conformation the bulky *tert*butyl groups of the (*M*) allene in the core induce the opposite twist into both neighboring TCBDs (Figure 3. 13). The simulated ECD spectra for this conformer at the (TD)-B3LYP/6-31G(d) level of theory is in good agreement with the experimental one, enabling the conformational assignment of (*M*)-**3** in solution. This geometry is very close the one found in solid state by X-ray.[17]

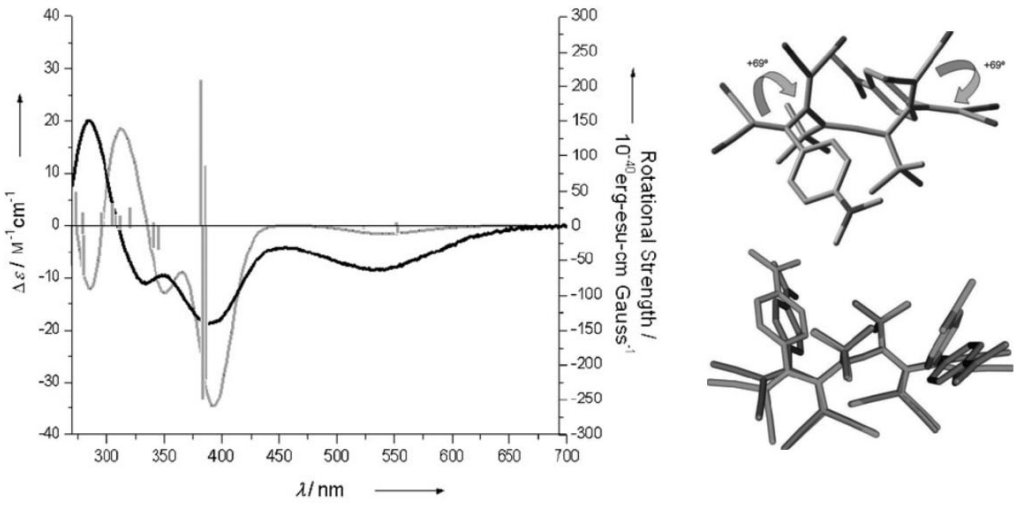

*Figure 3. 13 left: CD spectrum of (*M*)-**3** (recorded in CH_2Cl_2 (black line), calculated CD curve for (*M*)-**3b** at the TDDFT B3LYP/6-31G(d) level of theory (s=0.10, scaled to 1.0, gray line), and rotational strengths for the different transitions (gray bars).*[10] *right top: global minimum-energy conformer (*M*)-**3b** obtained via B3LYP/6-31G(d) geometry optimization; arrows show positive conformational helicity across both TCBDs. right bottom: Overlay of the geometry for the global minimum (*M*)-**3b** (B3LYP 6-31G(d)) and the geometry obtained from X-ray crystallographic analysis (CCDC-691333).*[17]

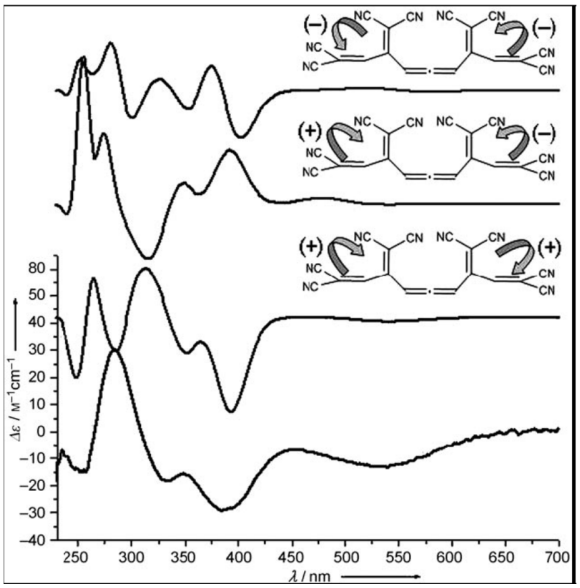

*Figure 3. 14 From top to bottom: calculated CD curves for (*M*)-**3n**, (*M*)-**3i**, and (*M*)-**3b** (s=0.10, scaled to 1.0) at the TDDFT B3LYP/6-31G(d) level of theory, and CD spectrum of (*M*)-**3** recorded in CH_2Cl_2.*[17]

In order to verify the reliability of ECD for the conformational assignment of (*M*)-**3**, the ECD of conformers (*M*)-**3i** and (*M*)-**3n**, which have an opposite twist for one and two TCBD moieties respectively compared to the global minimum, were simulated and compared with the experimental ECD for (*M*)-**3** in CH_2Cl_2 and predicted ECD for (*M*)-**3b**. As it is shown in Figure 3. 14, in this case-study, the circular dichroism is very sensitive to small conformational changes, underlining the reliability of this method for the conformational assignment.

3.4.4. **Challenge due to vibronic coupling**

Vibronic coupling originates from the interaction between vibrational and electronic transitions. Often this phenomenon hampers the correct prediction of UV/Vis and ECD spectra by simply considering electronic transitions. Particularly, molecules bearing acetylene groups typically present fine structures in the UV/Vis spectra with spacing between the bands of ca. 2200 cm^{-1}, corresponding to the vibrational frequency of the acetylene bond stretch.

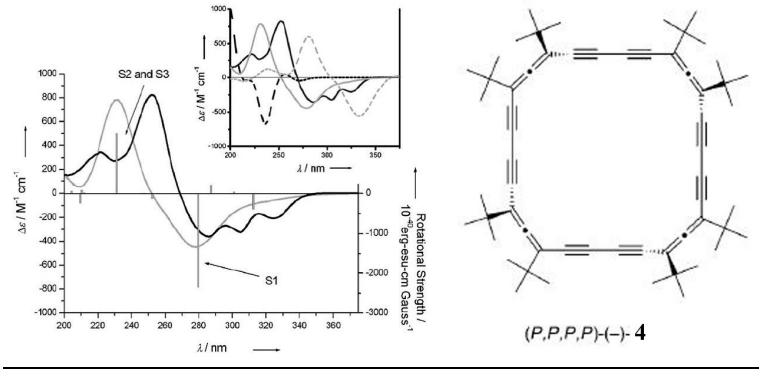

*Figure 3. 15 Experimental (black line) and simulated CD spectrum of (*P,P,P,P*)-(–)-**4** (gray line, scaled by 0.6, not shifted, rotational strength in gray bars) at the CAM-B3LYP/6-31G(d) level of theory. The inset shows experimental (black line) and simulated CD spectrum of (*P,P,P,P*)-(–)-**1** at the HF/6-31G(d) (dashed black line scaled by 0.2, not shifted), ZINDO (dashed gray line scaled by 0.4, not shifted), and CAM-B3LYP/6-31G(d) (gray line scaled by 0.6, not shifted) levels of theory.*[19]

As an example, the shape persistent alleno–acetylenic (*P,P,P,P*)-(–)-**4**,[20] presents a strong vibronic coupling in the ECD (Figure 3. 15). Both, the system size and the presence of high density of states around the transition originating the vibronic coupling, unable the prediction of the fine structure present in the UV/Vis and ECD. However, when comparing the theoretical ECD spectra at different levels of theory without considering the vibronic coupling with the experimental one, the overall agreement allows the AC elucidation of this complex system.[19]

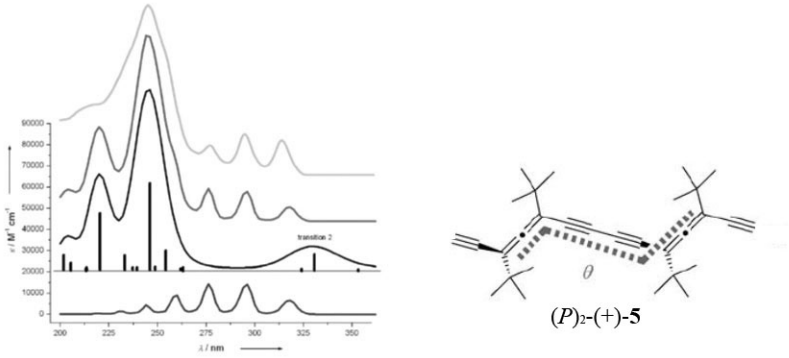

*Figure 3. 16 Franck-Condon prediction for transition 2 at the HF/6-31G(d) level of theory (blue-shifted 0.05 eV, σ = 0.07, scaled by 2.0). Black line: calculated electronic UV/Vis (20 vertical transitions represented by black bars were calculated at the HF/6-31G(d) level of theory, blue-shifted 1 eV, σ = 0.2, scaled by 3.0). Gray: summation of the FC trace and the electronic UV/Vis trace excluding the transition 2. Light gray: experimental UV/Vis spectrum (n-hexane) of (*P*)₂-(+)-**5**. These calculations were performed on (*P*)₂-(+)-**5** with θ = +45° with tert-butyl groups substituted by protons.*[21]

On the other hand, Franck-Condon calculations on the simpler system presented in Figure 3.16 could successfully reproduce the experimentally observed vibrational progression bands. This phenomenon splits the electronic transition at 330 nm into several vibronic bands. The good agreement of experimental and theoretically predicted spectra was used for the conformational preference of acyclic chiral oligomers in solution.[21]

3.5 Vibrational Circular Dichroism (VCD)

VCD method, with the first reported measurement dating to year 1974[22], represents the youngest analogue of the CD-based spectroscopy. It originates from vibrational transitions within the ground electronic state of a molecule, triggered by the infrared (IR) domain of circular polarization. The appreciation of VCD spectroscopy as a method for the reliable AC assignment has increased exponentially in the past four decades, as evidenced by the corresponding increase in the number of successful reported cases.

The basic considerations needed for carrying out a VCD measurement are as follows: The criterion which dictates the combination of the sample concentration and pathlength used in an experiment is the need for Vibrational Absorption (VA) band to be in range 0.2-1 (absorbance units). Typical sample concentrations required are 1–50 mg/mL, with volumes ranging from 30–100 µL needed to fill-up the 25–100 µm pathlength cell. The typical solvents used are CCl_4, CS_2, CH_3OH, $CHCl_3$, CH_2Cl_2, CH_3CN, DMSO, H_2O and often, their deuterated analogues. The listed pool of solvents is considered to be relatively IR "silent". The solvent choice is dictated by the need for minimal interference of solvent's absorption in the frequency region of anticipated vibrational normal modes of the sample. Deuturated samples are beneficial for shifting away the solvent band that could be potentially interfering with sample bands (i.e. strong hydroxyl group bending modes of H_2O at ~1500cm^{-1} are shifted to 1250cm^{-1} in the case of D_2O).

The IR region of electromagnetic radiation spans three sub-regions: near-IR, mid-IR, and far-IR. Upon absorbing mid-IR radiation (800–4000cm^{-1}), functional groups within a molecule engage in normal modes (stretching and bending motions). Since mid-IR region arises from fundamental vibrational normal modes that can be reliably predicted via *ab initio* calculations, this region is the best choice for determining molecular stereochemistry. Despite the fact that VCD activity can be experimentally detected in the near and far-IR regions, at this point in time the available levels of theory do not allow accurate predictions of overtones and combination bands.

Similarly to UV and ECD intensities, the theoretical quantities appropriate for VA and VCD intensities of normal modes are dipole strength (*D*) and rotational strength (*R*), respectively. The Lorentzian band-shape is used for simulating the VCD trace with bandwith of ~ 6–10 cm^{-1}. Typically global scale factors (i.e. 0.9613 for 6-31G* basis set) are applied to compensate for the harmonic overestimation of the simulated frequencies.

In the qualitative interpretation of VCD spectra, the correct signs of the *R* parameter are crucial when assigning AC, while the accuracy of the magnitude of the *R* is less important. For the purpose of determining the AC, it is sufficient to compare predicted and experimental mid-IR VCD

sings on a qualitative level. However, if an additional goal is to determine the populations of individual conformers, then quantitative comparison is desirable.

In the past few years, several VCD studies have emphasized the importance to establish an intrinsic measure for identification of overly sensitive, and, hence, unreliable theoretical VCD bands. Two such recently developed methodologies include robustness concept and ζ-factor analysis.[23][24][25][26] According to robustness definition, if the angle between electric and magnetic dipole transitions moments is close to 90º (±30º), then a given band is not to be considered robust, which means that it is not reliable. Furthermore, in a recent report, Gobi *et al*.[6] have suggested that if the magnitude of the so-called ζ-factor ($\zeta = R/D$) is below 10 ppm, the associated band can be disregarded from the correlation. Even though both analyses have been recently applied in investigations of a few chiral systems, these reliability gauges have not yet been widely tested and verified in terms of suitability for broad application.[27]

Most recently, a new robustness criterion has been suggested[28] to be applied not only to calculated VCD and VA spectra, but also to the experimental analogues. This newest method, based on so-called dissymmetry factor as imposition of robustness, seems to have potential to be the most practical as it considers robustness of regions of the VCD spectra rather than robust of individual transitions. Certainly, future publications will show which method serves as the most practical quantitative measure of the simulated-experimental correlations within the VCD spectroscopy in order to increase the confidence level of the AC assignment.

3.5.1 Advantages of VCD

- The investigated chiral molecules do not need to have any chromophoric groups, as every vibrational normal mode is a potential chirality probe. For nonlinear molecule with N atoms there are 3N-5 normal modes, each of which could be structurally diagnostic. As a consequence, VCD spectra typically have a richer structural content and hence AC assignment involves correlation of multiple bands.
- In contrast to NMR which yields weighted averages for fast molecular movements, VCD detects each species present as a linear combination of all contributing conformers. Therefore, in the case of more flexible molecules, the higher spectral resolution of VCD allows simultaneous elucidation of configuration and conformation.
- Reliable theoretical support is another advantage of VCD methodology. Namely, *ab initio* predictions of VCD are typically reliable as they are within ground electronic state with a much lower probability for incorrect interpretations.

3.5.2 Limitations of VCD

- VCD probes chirality less efficiently compared to ECD, since the signals are ~ three-four orders of magnitude smaller.
- In the case of VCD, the chiral susceptibilities for nuclear vibrations are considerably smaller than the corresponding signals in the UV/Vis range. Competition of such weak effect with largely fluctuating indecent IR beams is the reason why it typically takes 1-3 hours data accumulation time to acquire statistically meaningful VCD spectra.
- Detectors are inherently less sensitive than the ones used in ECD methodology. As a result the acceptable signal-to-noise ratio mandates not only longer accumulation time, but also higher concentration (1–50mg/mL).

Nevertheless, the advantages have outweighed the disadvantages and VCD has acquired status of a reliable and convenient tool for determining molecular stereochemistry.

3.5.3 Application of VCD

Four levels of complexity can be encountered during the AC assignment of chiral molecules as tackled by VCD spectroscopy:

- Unambiguous AC assignment of moderately flexible molecules with one chiral center
- Unambiguous AC assignment of flexible molecules with more than one chiral center
- Establishing solute-solvent & solute-solute intermolecular interactions of chiral molecules
- AC assignment via VCD exciton coupling methodology, the future perspective

It should be noted that the utility of VCD provided in examples that follow is frequently, yet not universally applicable.

3.5.3.1. Unambiguous AC assignment of moderately flexible molecules with one chiral center

An example of a molecule with moderate conformational flexibility endowed with a single chiral center is an isolated chromane presented in Figure 3. 17.[29] The survey of the potential energy surface (PES) has been initially simplified by performing molecular mechanics conformational search on the fragment-molecule. Conformers within 6 kcal mol^{-1} energy window have been subjected to geometry optimization at the B3LYP/6-31G(d) level of theory. Among the 54 conformers calculated, 11 (each with Boltzmann population > 2%) were selected to build-up the whole molecular model.

After full geometry optimization, four lowest-energy conformers with an overall 80% Boltzmann population were considered for the VCD calculations.

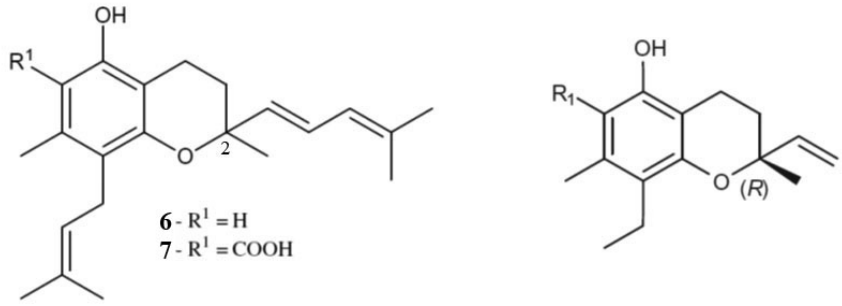

*Figure 3. 17 Structure of chromane **6** isolated from leaves of Peperomia obtusifolia and its fragment analogue **7** used for more efficient conformational search.*[29]

The predicted VCD spectra for the individual conformers are presented in Figure 3. 18, while correlation between experimental and Boltzmann averaged theoretical spectra are presented in panel b) of the same figure. It is worth noting that differences in the VCD spectral traces among the four most stable conformers exemplify the capability of VCD to distinguish and hence identify the different conformers present in solution. Specifically, VCD unveils that the bulky isoprenoid chain at C-2 preferentially adopts the axial position. The confidence level for the assignment of (+)-**6** to (*R*)-**6** with (*P*)-helicity of the chromane ring is reflected in highly satisfactory correlation between multiple experimental and theoretical VCD bands.

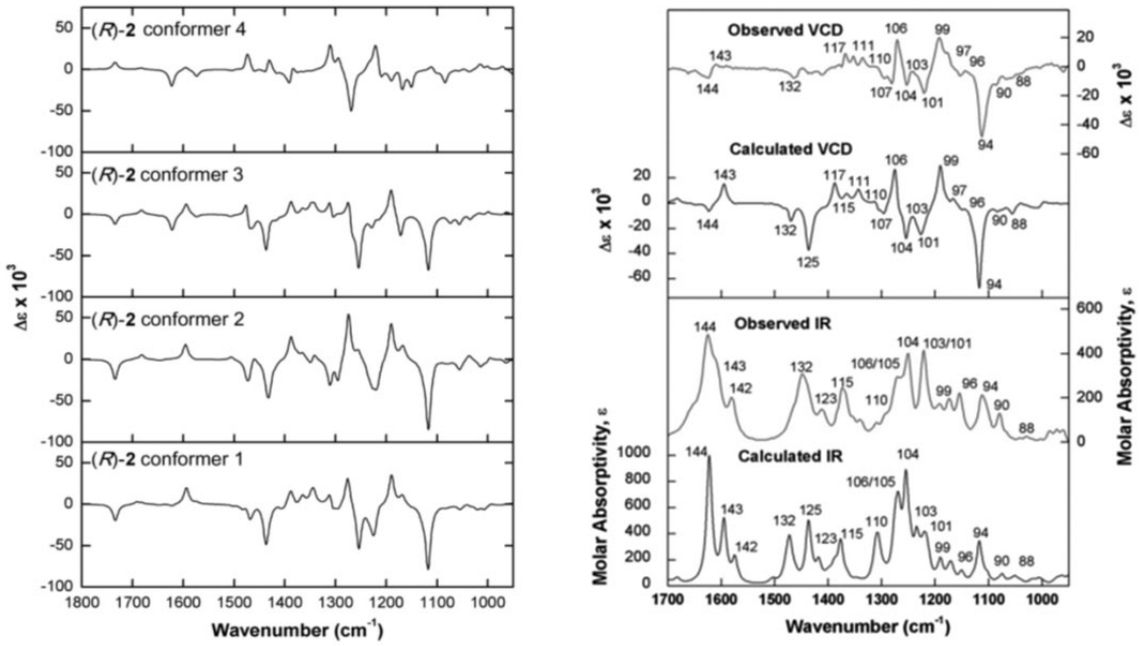

*Figure 3. 18 Panel a) displays calculated VCD spectra for four stable, low energy conformers. Panel b) provides comparison of VA and VCD spectra measured for (+)-**1a** with the analogous calculated sepctra of the Boltzmann average of the four lowest-energy conformers of the* (R)-***1.***[29]

In the present case study, VCD serves as a reliable probe of both the AC and predominant conformers in solution. It should be noted, however, that in less prominent cases, VCD can suffer from the existence of too many conformers.[30][31] Few studies, such as VCD based investigation of 1,2 and 1,3-diols, have engaged in chemical "rigidification" of the mobile groups to amplify the VCD signals and hence provide a unambiguous AC analysis.[32]

3.5.3.2. Unambiguous AC assignment of flexible molecules with more than one chiral center

VCD displays a capacity to reliably distinguish between diastereomers. Compound **8** is also chromane-based as **6**, yet a closer inspection of its structure (Figure 3. 19) promptly suggests two reasons for a higher level of complexity in assigning the AC then the previous case study: first, the presented monoterpene chromane ester[33] is endowed with more than one chiral center; second it exhibits considerable conformational flexibility, implying that each of the diastereomers could possibly have several conformations. The lack of UV/Vis chromophores within the monoterpene moieties makes VCD the best choice for the structural characterization.

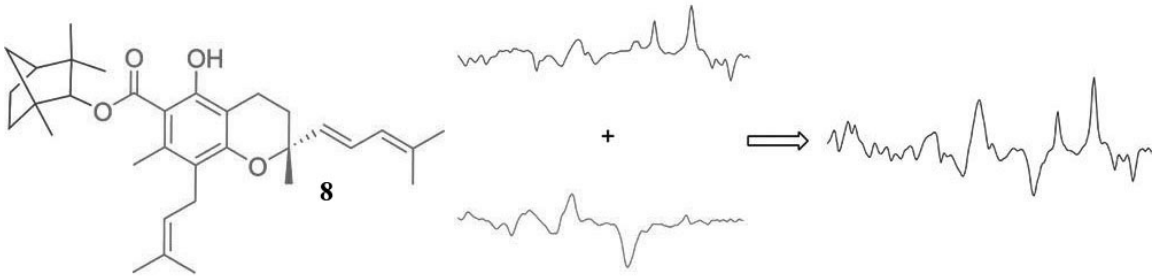

*Figure 3. 19 Structure of monoterpene chromane ester **8** isolated from leaves of Peperomia obtusifolia along with VCD spectral traces as localized responses of monoterpene vs. chromane segments of the molecule.*[33]

Once the relative stereochemistry has been assessed for monoterpene segment (1'", 2'", 4'") via NMR, the VCD-based challenge was to establish the relative stereochemistry at C-2 and subsequently determine the AC at each of the four chiral centers. Figure 3.20 presents a very good agreement between the spectra of one of the (+)-diastereomes and those calculated for (2R, 1'"S, 2'"R, 4'"S) using two levels of theory. A thorough spectral analysis unveils the presence of localized VCD features that can be assigned to the monoterpene and chromane motifs separately, while other bands predominantly result from vibrations involving the rest of molecular frame. For example, VCD bands labeled 101, 103, 111, and 116 (Figure 3. 20) are due to vibrations localized within the monoterpenes and permit the identification of AC within this segment of the molecule. On the other hand, the VCD bands designated as 122 and 130, serve as a diagnostic markers for the configuration at C-2. Specifically as it pertains to the AC at C-2 chiral center, it has been noted that a negative and positive combination of 122 and 130 bands respectively accounts for the (*R*) configuration, whereas the opposite corresponds to (*S*).

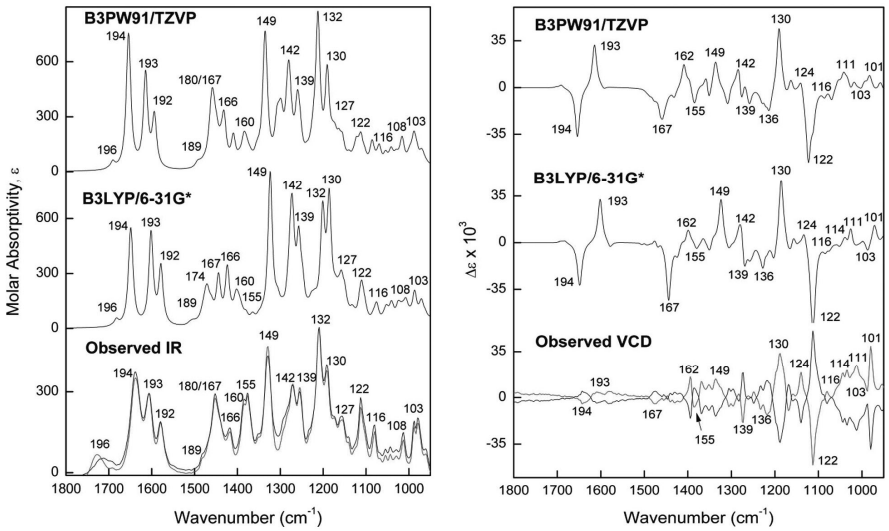

*Figure 3. 20 Panel displays a) comparison between experimental and calculated VA; Panel displays b) comparison between experimental and calculated VCD, respectively for (+)-**8** and (2R, 1'''S, 2'''R, 4'''S); Calculated data are presented for two levels of theory.*[33]

Finally, if the relative configuration of the molecule under study is unknown, one should simulate the VCD spectra for all possible diastereomers. It is worth mentioning that half of diasteromers provide mirror image spectra of the other half, hence only the first half requires VCD simulations and the VCD for the other half can be obtained by multiplying the intensities by (-1). The precaution of considering the VCD of all diastereomers insures that the satisfactory spectral resemblance with experimental spectra is displayed by only one theoretical model of a given AC.

3.5.3.3. Establishing solute-solvent & solute-solute intermolecular interactions of chiral molecules

In recent years, VCD has opened new horizons for identifying and monitoring intermolecular interactions, primarily of H-bonding and van der Waals variety. Such investigations can be grouped into two categories: a) studies of chiral induction of solvent due to solute-solvent interaction and b) studies which enable monitoring dimer, trimer or high-order complex formation due to solute-solute interaction. For each category, representative studies have been selected to illustrate the relevance of VCD in providing the spectral fingerprint of intermolecular interactions.

a) Solute-Solvent Interactions: The newest findings demonstrate that the VCD modes of the non-chiral solvent molecule acquire significant rotational strengths upon forming H-bonding with a chiral solute. It was additionally found that the VCD spectra of different solute-solvent conformers often exhibit not only different shapes but also different signs reflecting the geometry of the complex. These generic changes in spectral features allow VCD spectroscopy to serve as a conclusive interpretation tool of the specific types of solute-solvent interactions.

VCD investigation of interaction between D-lactic acid and water demonstrates the above stated utility.[27] It was found that the lactic acid monomer is not the dominant form in the solution and that the clusters of lactic acid and water best reproduce the experimental VCD spectra.[34,35]

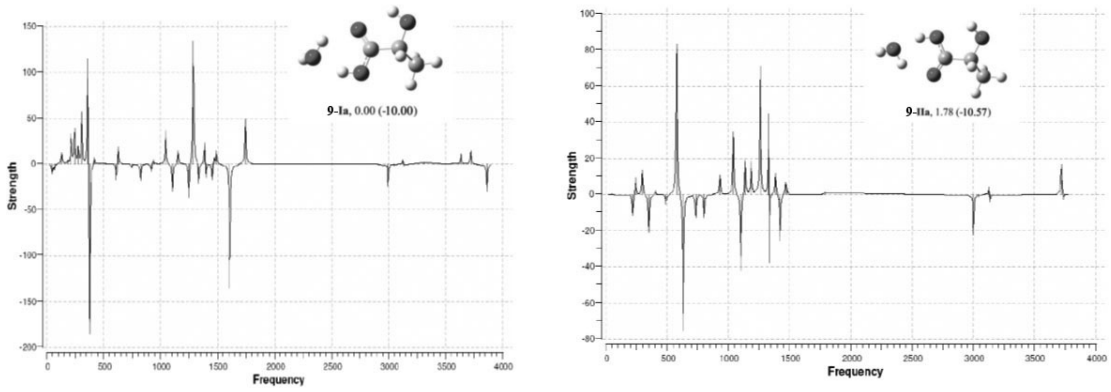

*Figure 3. 21 Calculated VCD spectra of the two stable solute-solvent conformations **9-Ia** and **9-IIa** displaying H-bonding interaction between D-lactic acid and water.*[35]

The calculated VCD spectra (Figure 3. 21) of two different solute-solvent complexes demonstrate the ability to discern the characteristic spectral patterns associated with specific configuration of intermolecular H-bonding in the lactic acid-water complexes: i) Upon complexation, a non-chiral water molecule acquires a VCD signal with significant rotational strength, specifically notable for bending modes at ~1550cm^{-1}; ii) The sign in rotational strengths of one of the two stretching modes of water at ~3400cm^{-1} is opposite for both conformers, which demonstrates that VCD can be used as a discerning marker of the two H-bonding conformations; iii) Besides the opposing sign of the stretching band, the intensity maximum of this band also exhibits a 30 cm^{-1} difference in frequency. This frequency-based distinction is observable through VCD, but hardly observable through IR intensities.

Finally, it can be noted that theoretical VCD studies on even more complex models of lactic-acid and water have been attempted. As it can be seen from Figure 3. 22, the stretching OH mode from COOH at 3315 cm^{-1} and at 3292 cm^{-1} has a different VCD sign and hence represents a diagnostic band between the two solute-solvent complexes.[35]

In conclusion, since solute-solvent intermolecular interactions can even change the sign of some VCD transitions, the spectral interpretation has to be done with care. The strategy could be two-fold: either intermolecular interaction effects have to be accounted for in the quantum mechanical treatment of VCD spectra or the intermolecular interactions during the VCD measurements have to be eliminated or at least minimized. From experimental perspective, one could choose to select weakly interacting solvents to stabilize the monomeric form of a chiral solute. If the solubility allows, the formation of solute-solvent interactions can be avoided by resorting to CCl_4 or other apolar solvents.

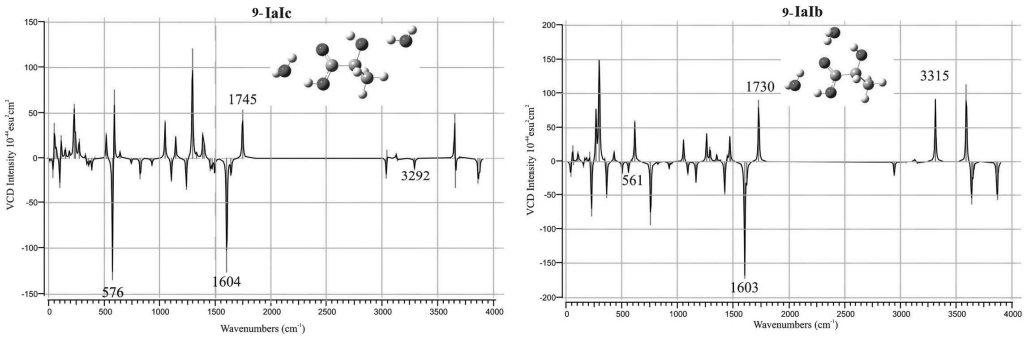

*Figure 3. 22 Calculated VCD spectra of the two trimer conformations **9-IaIb** and **9-IaIc** of lactic acid---(water)$_2$.*[35]

In some cases, satisfactory estimation of the solvation effects on VCD spectra can be determined using implicit solvent models, such as previously mentioned polarizable continuum (PCM, IEF-PCM) models. One way to rule-out necessity for accounting for solute-solvent interactions is to make measurements in polar ($CHCl_3$) and apolar (CCl_4) media. This is conditioned by the ability to dissolve the sample of interest in both solvent media. The implicit solvation model is sufficient if the spectra display no significant differences between solvents such as CCl_4 and $CHCl_3$.

b) Solute-Solute Interactions: The notion that VCD spectra can potentially be used to better characterize the intermolecular solute-solute interactions (dimer, trimer, or even higher complex formation) comes naturally for this technique due to a need for higher sample concentrations.[11] If bulky groups do not inhibit the intermolecular solute-solute or solute-solvent interactions, comparison of the predicted spectra of the complexes with the experimental spectra recorded in relatively concentrated solutions is mandatory.

A recent case study in which the solvated dimer had to be accounted for is that of (S)-α-phenylethyl isocyanide (PENC, (*S*)-**10**) in chloroform.[36] As it can be seen from Figure 3. 23, PENC is a small chiral molecule with only one relevant conformational degree of freedom associated with the phenyl moiety. According to the conformational search and geometry optimization analysis, there is only one conformation significantly present in solution.

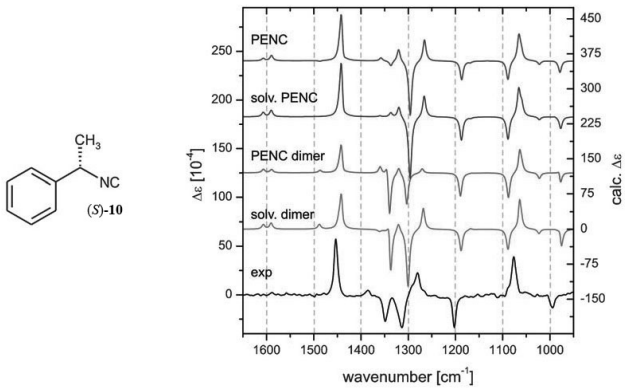

*Figure 3. 23 Comparison of the experimental VCD for (*S*)-**10** with VCD calculated for the isolated monomer, solvated monomer, dimer, and solvated dimer.*[36]

The results of the spectra calculations for the energetically favored conformer are compared to the experimental spectra in **Erro Non se atopa a orixe da referencia.**. Considering the fairly rigid nature of the small molecule in this case study, the experimental VCD spectra show only partially good agreement with calculated VCD for the monomeric form of (*S*)-**10**. There are two VCD segments that are not correlated with the calculations. In particular, these are the negative peaks around 1100 cm^{-1} and the pattern between 1400–1300 cm^{-1}. In search for better spectral correlation, the authors have taken into account implicit solvent model, explicit solvent model, dimer and explicitly solvated dimer (Figure 3. 24). VCD pattern arising from VA bands located at ~1330 cm^{-1} change dramatically when going from the monomer to the dimer. Thus, the introduction of the dimer and especially explicitly solvated dimer definitely serves as an improvement.

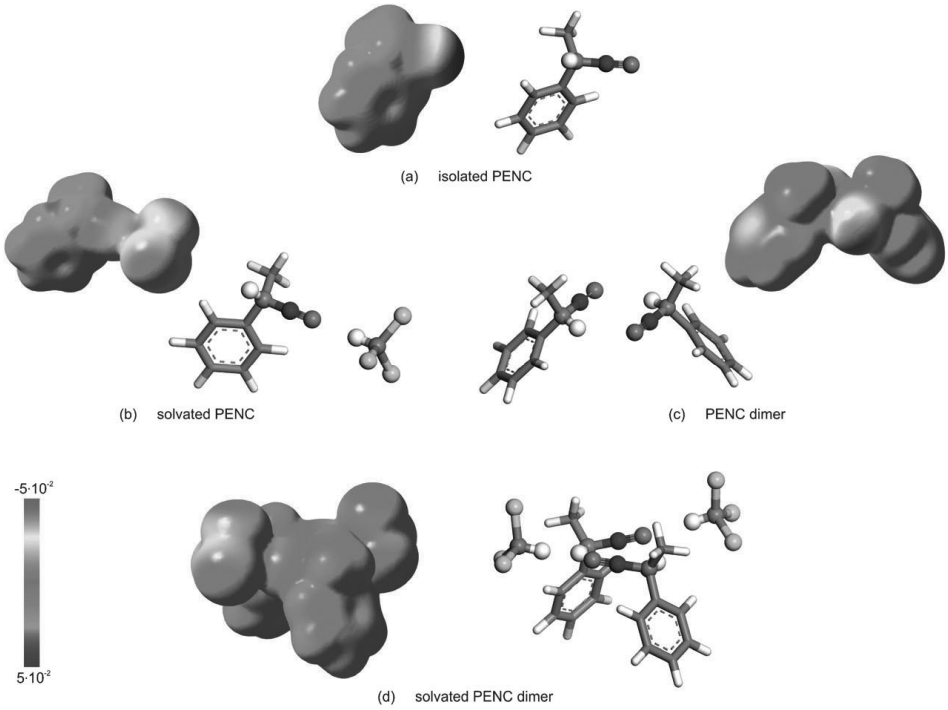

*Figure 3. 24 Molecular electrostatic potential mapped on the total electron density distribution for a) (S)-**10** monomer, b) solvated monomer, c) dimer and d) solvated dimer.*[36]

The VCD spectrum of α-phenylethyl isocyanide in chloroform is one of the few examples for which both solute-solute and solute-solvent interactions have to be taken into account in order to obtain a good theoretical description of its structure in solution.

3.5.3.4. AC assignment via VCD exciton coupling methodology, the future perspective

The most recent advance in applying VCD to establish AC has been to employ the exciton coupling method in the IR-regime, which is an intriguing idea proposed by Taniguchi et al.[37] Similarly to ECD based exciton coupling methodology, bisignate VCD couplet originates from two chiral moieties. For example, camphor derived β-diketon analogues (Figure 3. 25) qualify for VCD exciton coupling method.

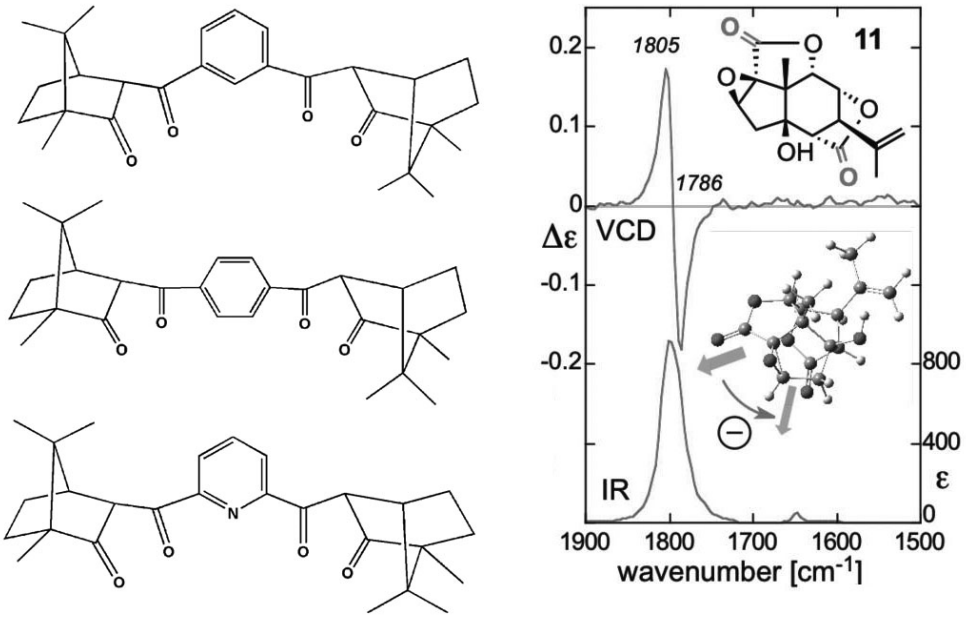

Figure 3. 25 left: provides structures of β-diketon analogues which are suitable for VCD exciton couplet method; right: provides VA and VCD exciton couplet response for compound ***11***.[37,38]

VCD exiton couplet signals analyzed for a series of small molecules with two IR active groups lead to the recognition of two appealing prospects for applying the methodology:[37,38] a) It bypasses the need for expensive theoretical simulations as current evidence shows that experimental signals can be used for fast analysis of AC even if the overall molecules exhibits various conformations; b) The intrinsically weak VCD signal (ex. carbonyl band region ~1750 cm^{-1}) is amplified by factor of ~20. This further translates into an advantage that the sample amount for the detection of VCD can be lowered by the exciton coupling effect. Overall, the proposed VCD exciton coupling method awaits further validation of its scope with future investigations.

3.6 Optical Rotatory Dispersion (ORD)

Optical rotation is the oldest of the chiroptical methods. Traditionally optical rotation was measured at the sodium D line (λ=589 nm) to provide the $[\alpha]_D$ values. However, the optical rotation can be measured at different wavelengths, and as such, it is referred to as optical rotatory dispersion (ORD). The specific rotation of a solution is expressed as $[\alpha] = 100\alpha / lc$, where α is the measured optical rotation at a certain λ, l is the path length in dm and c the concentration of the sample in g per 100 mL of solution. The specific rotation is often used to determine the enantiomeric purity of

a sample. It has also been used for the AC determination of several molecules using empirical rules. As mentioned for ECD, nowadays it is not recommended of solely rely on empirical rules but rather to compare experimental and theoretically predicted optical rotations. The optical rotation is very easy and quick to measure, typically 1 to 10 mg of sample solubilized in about 1 mL of solvent. However, the rather high concentrations employed can favor the formation of solute-solute interactions that may increase the complexity of the analysis. To exclude the presence of this interference, measurements at different concentrations should be measured. The specific rotation at very small concentrations is called intrinsic rotation.[39] Chiroptical responses at low concentration are principally induced by an individual molecule and therefore those values are appropriate to be compared with the theoretically predicted intrinsic rotation.

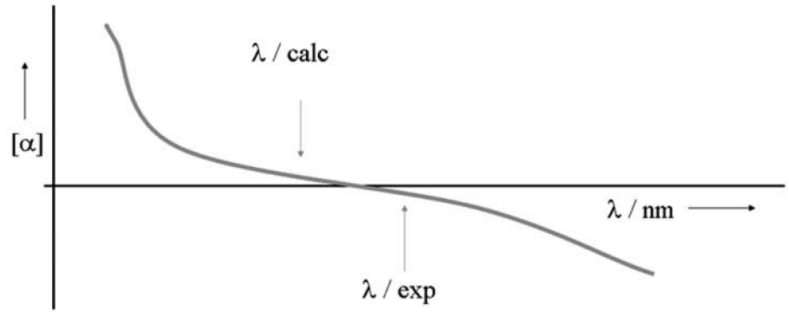

Figure 3. 26 Representation of optical rotation at different wavelengths.[40]

In the last decades, the development in computational chemistry has considerably improved the reliability in the predicted optical rotations. However, as it often happens in ECD and VCD, certain inaccuracy in the prediction of the energy of the transitions may provide the theoretically predicted OR values with energy shift with respect to the experimental ones. This is the reason why ORD analysis is strongly recommended instead of simply relying on a single wavelength OR. Typically, a qualitative comparison between experimental and theoretical ORD curves is based in the signs and curvatures (overall trend). When using several wavelengths, an energy shift in the theoretical ORD prediction will not drive to an improper assignment. However, when a single OR is considered, an energy shift could drive to an incorrect assignment (Figure 3. 26).[40] As it can be seen if Figure 3.26, the OR could be measured at λ/exp providing a negative signal, while the shifted theoretical prediction at λ/calc could provide a positive signal. A circumstance of considering only a single wavelength (λ) value of OR would likely result in a wrong AC assignment.

3.6.1 Advantages of ORD

- No presence of UV/Vis active chromophores is needed.

- ORD can be easily implemented in the available ECD spectrometers.
- Very fast and easy to measure.
- Not affected by vibronic coupling.

3.6.2 Limitations of ORD

- The theoretical simulation of the spectra needs the prediction of electronic excited states.
- The low signal resolution makes ORD not suitable for flexible molecules with opposite responses for different conformers.
- Between 1 mg and 10 mg of sample is needed.

Regularly ORD is chosen as a cross validation method when ECD and/or VCD are not unambiguous. The use of a particular chiroptical method should be taking into account based on the nature as well as the amount of material in hand. However often, the use of more than one method is required, or at least recommended as a cross-validation for structure determination of challenging chiral molecules.[16, 17]

3.7 When more than one method is needed

Despite that each invididual method carries the capacity for independent stereochemical structural elucidation, in some cases comibination of more than one method is desirable for two key reasons: a) to increase the confidence level of the AC and conformational assignment, b) to bypass limitations of a given method either with respect to certain classes of chiral compounds or the experimental conditions. The text below provides examples of case studies in which tandem application of more than one chirotpical method was desirable and in some cases necessary.

3.7.1 Combination of ECD and VCD

The tripodal cyclotriveratrylene (CTV) (*M*)-**12** and its enantiomer were prepared on a study to perform regioselective additions to C_{60} (Figure 3. 27).[41]

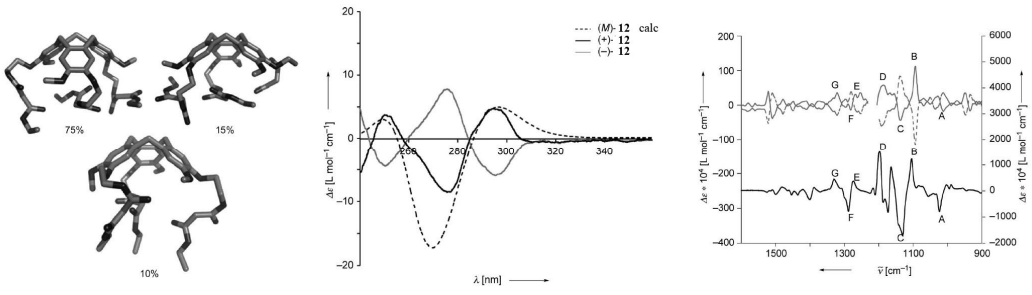

*Figure 3. 27 Left: low-energy conformers of (M)-**12** and their relative populations in a Boltzmann ensemble. Center: Experimental ECD spectra (CH_2Cl_2) of CTV-derived trimalonates (+)-**12** (black solid line) and (–)-**12** (gray solid line), and the spectrum calculated for (M)-**12** [TD-B3LYP/6-31G(d) (black dashed line). Right: Experimental VCD spectra (0.042 M, CCl_4) of (+)-**12** (gray solid line) and (–)-**12** (gray dashed line), and the VCD trace calculated for (M)-**12** (black solid line). The calculated frequencies were scaled by the basis-set-specific factor 0.97. The region between 1200 and 1240 cm^{-1} is omitted due to intense solvent (CCl_4) absorption.*[41]

The AC of (+)-**12** was fist assigned the same as a known derivative of a precursor. However, the low energetic barrier isomerization of these cyclotriveratrylenes calls for the use of chiroptical methods in order to ascertain the AC assignment.[41] The PES of (+)-**12** was explored using the force field MMFF implemented in MacroModel 9.5, followed by the optimization of the non-redundant conformers at the B3LYPT/6-31G(d)//AM1 level of theory (this notation means that first the optimization was performed at the AM1 followed by the B3LYPT/6-31G(d) levels of theory). The resulting three conformers are presented in Scheme 3.27. The ECD spectrum was measured and simulated using TD-DFT. The Boltzmann-weighted spectra of the three conformers resembles very well the experimental ECD of (*M*)-**12**, therefore, confirming the AC of (+)-**12** as (*M*)-**12**. As a cross-validation, the Boltzmann-weighted VCD spectra of all conformers was also found to resemble very well the experimental one, therefore being in agreement with the ECD results (Scheme 3.27).[41]

3.7.2 Combination of ECD and ORD

Oligomers from dimer to hexadecamer were synthetized from enantiopure allenes with known AC and the ECD as well as ORD intensities showed no linearity with the number of building blocks. This observed chiral amplification suggested the formation of ordered structures in solution.[21]

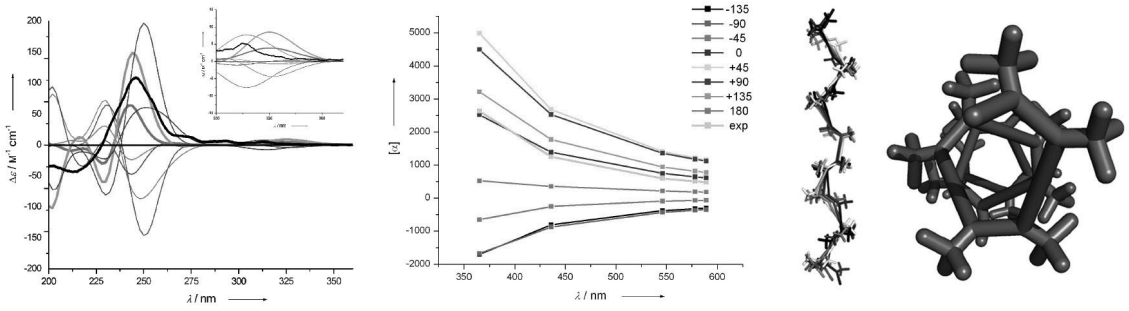

*Figure 3. 28 Left: CD spectra of $(P)_2$-(+)-**5** at θ = –135°, –90°, –45°, 0°, +45°, +90°, and 180°, calculated at the TD HF/6-31G(d) level of theory. Experimental spectrum of $(P)_2$-(+)-**5** (black thick line). The inset is an expansion of the region between 350 and 300 nm. Center: Calculated ORD and experimental (chloroform) traces of $(P)_2$-(+)-**5** at the HF/6-31G(d) level of theory. Right: Ensemble of four helical conformers of $(P)_8$-(+)-**5** in the 0° ≤θ≤ +45° range and view along the helix axis of the conformer at θ = 0°.*[21]

These alleno-acetylenic oligomers, in addition to the vibronic coupling mentioned above, present an additional challenge: the low rotational barriers about the butadiene moieties hampering the definition of a PES. As an alternative, the ECD and ORD spectra of $(P)_2$-(+)-**5** with different conformations about the central single bond were simulated and compared with the experimental ones (Figure 3. 28). The ORD analysis, at the HF/6-31G(d) level of theory, suggested that the conformers in solution should have a θ in 0° to +135° range. The comparison of the experimental and theoretical ECD spectra allowed narrowing the conformational space in 0° to +45° range. ZINDO, HF/6-31G(d), and B3LYP/6-31-G(d) levels of theory provided similar ECD signatures for a particular conformer.

3.7.3 Combination of VCD and ORD

The chiral trailkynyl(phenyl)-methane (*R*)-**13** was obtained from the resolution of its racemate as a precursor of expanded cubanes.[42] Due to the lack of strong electronic transitions in the UV-Vis region, the ECD signals are very weak and not suitable for the AC determination. Therefore, the combination of VCD and ORD analysis was considered. First, the conformational search was performed in order to define the PES. The resulting geometries were optimized at the B3LYP/6-31G(d) level of theory rendering three main conformers (Figure 3. 29).

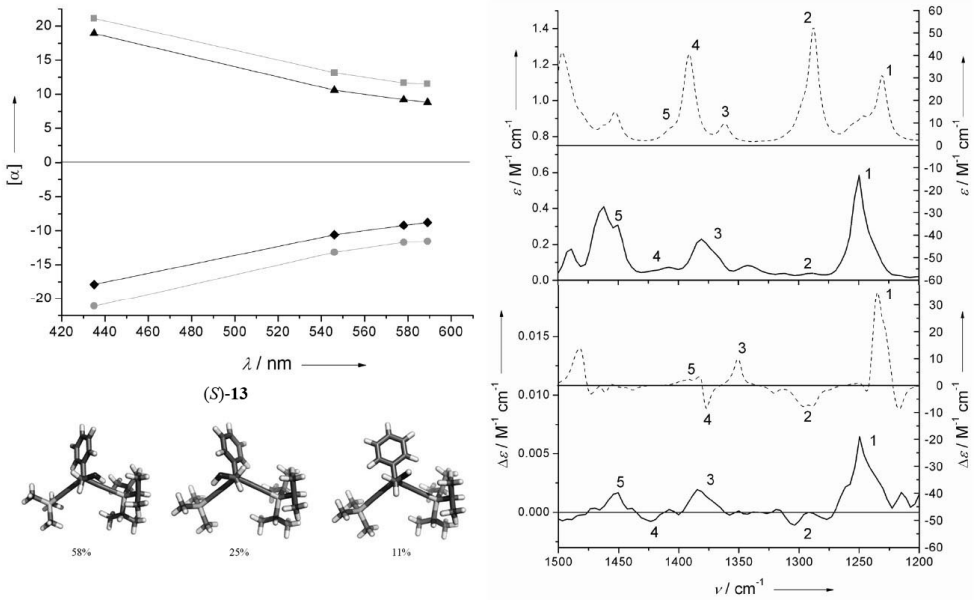

*Figure 3. 29 Left top: Experimental ORD curves of (+)-**13** (c = 9.6 mM in hexane, triangles, black line) and (–)-**13** (c = 12.5 mM in hexane, diamonds, black line). Calculated ORD values at the B3LYP/6- 31G(d) level of theory for (R)-**13** (squares, gray line) and (S)-**13** (circles, gray line). The theoretical values were adjusted by scaling down by a factor of 0.3. Left bottom: Conformers of (R)-**13** found at the B3LYP/6-31G(d) level of theory. The conformer populations (Boltzmann distribution) were determined by using the computed Gibbs free energy at 298.15 K. Right: Calculated IR (dashed line, upper graph), experimental IR (solid line, upper graph), calculated VCD (dashed line, lower graph), and experimental VCD spectrum (solid line, lower graph). Calculated frequencies were shifted by 0.97.*[42]

The Computed Gibbs free energy of the three conformers was used to determine the relative population in solution. The VCD and ORD spectra of all conformers were calculated at the B3LYP-6-31G(d) as well as B3PW91/6-31G+(d) levels of theory. The VCD simulated spectra of (*S*)-**13** (Boltzmann averaged of all three conformers, Scheme 3.29) has been compared with the experimental VCD of (–)-**13**. Predicted Cotton effects 1 and 2 resemble well the experimental ones. More importantly, these Cotton effects have the same sing for the three conformers, and therefore the average simulated signs do not depend on possible errors in the conformational analysis. Overall, the theoretical spectrum resembles qualitatively the experimental one. Nonetheless, the sign of Cotton effects 3, 4, and 5 is dependent on the conformation. In order to confirm the AC assignment made by VCD, the ORD of both enantiomers of **13** was measured at four different wavelengths. Now, the comparison of experimental and theoretical ORDs allows to unambiguously assign the AC of (–)-**13** as (*S*), in agreement with the VCD analysis (Scheme 3.29).[42]

In Chapter 11 an example of AC determination by a cross-validation of VCD, NMR and X-ray is also presented.

3.8 Concluding Remarks

Each chiroptical method (ECD, VCD and ORD) has its own unique advantages, and therefore, the choice of a particular method is case dependent. The rapid instrumental, methodological and theoretical developments in the last years have yielded notable improvements in the reliability of the AC as well as conformational assignments using these methods. Consequently, nowadays one can rely on the use of ECD, VCD, ORD, or a combination of them for structural determination of small and medium sized organic chiral molecules.

References

[1] T. D. Stephens, C. J. Bunde, B. J. Fillmore, *Biochem Pharmacol* **2000**, *59*, 1489–1499.

[2] P. J. Stephens, N. Harada, *Chirality* **2010**, *233*, 229–233.

[3] W. gaussian. co. Guassian 03 and 09., Gaussian Inc., Wallingford, CT 06492 USA, **2003**.

[4] T. D. Crawford, M. C. Tam, M. L. Abrams, *J Phys Chem A* **2007**, *111*, 12057–12068.

[5] N. L. Allinger, Y. H. Yuh, J. H. Lii, *J Am Chem Soc* **1989**, *111*, 8551–8566.

[6] S. Góbi, E. Vass, G. Magyarfalvi, G. Tarczay, *Phys Chem Chem Phys* **2011**, *13*, 13972–13984.

[7] N. Lin, F. Santoro, X. Zhao, A. Rizzo, V. Barone, *Society* **2008**, *4*, 12401–12411.

[8] W. Skomorowski, M. Pecul, P. Sałek, T. Helgaker, *J Chem Phys* **2007**, *127*, 085102.

[9] A. E. Aliev, Z. a Mia, M. J. M. Busson, R. J. Fitzmaurice, S. Caddick, *J Org Chem* **2012**, *77*, 6290–6295.

[10] B. Mennucci, J. Tomasi, R. Cammi, J. R. Cheeseman, M. J. Frisch, F. J. Devlin, S. Gabriel, P. J. Stephens, *J Phys Chem A* **2002**, *106*, 6102–6113.

[11] P. L. Polavarapu, *Chem Rec* **2007**, *7*, 125–136.

[12] V. P. Nicu, E. J. Baerends, P. L. Polavarapu, *J Phys Chem A* **2012**, *116*, 8366–8373.

[13] T. Kurtán, R. Jia, Y. Li, G. Pescitelli, Y.-W. Guo, *Eur J Org Chem* **2012**, *2012*, 6722–6728.

[14] N. Berova, L. Di Bari, G. Pescitelli, *Chem Soc Rev* **2007**, *36*, 914–931.

[15] N. Harada, H. Uda, *J Chem Soc, Chem Commun* **1982**, 230–232.

[16] J. L. Alonso-Gómez, P. Schanen, P. Rivera-Fuentes, P. Seiler, F. Diederich, *Chem Eur J* **2008**, *14*, 10564–10568.

[17] J. L. Alonso-Gómez, A. G. Petrovic, N. Harada, P. Rivera-Fuentes, N. Berova, F. Diederich, *Chem Eur J* **2009**, *15*, 8396–8400.

[18] J. G. Geist, S. Lauw, V. Illarionova, B. Illarionov, M. Fischer, T. Gräwert, F. Rohdich, W. Eisenreich, J. Kaiser, M. Groll, et al., *ChemMedChem* **2010**, *5*, 1092–1101.

[19] P. Rivera-Fuentes, J. L. Alonso-Gómez, A. G. Petrovic, P. Seiler, F. Santoro, N. Harada, N. Berova, H. S. Rzepa, F. Diederich, *Chem Eur J* **2010**, *16*, 9796–9807.

[20] J. L. Alonso-Gómez, P. Rivera-Fuentes, N. Harada, N. Berova, F. Diederich, *Angew Chem Int Ed* **2009**, *48*, 5545–5548.

[21] P. Rivera-Fuentes, J. L. Alonso-Gómez, A. G. Petrovic, F. Santoro, N. Harada, N. Berova, F. Diederich, *Angew Chem Int Ed* **2010**, *49*, 2247–2250.

[22] T. R. Faulkner, A. Moscowitz, G. Holzwarth, E. C. Hsu, H. S. Mosher, *J Am Chem Soc* **1974**, *96*, 252–253.

[23] E. De Gussem, P. Bultinck, M. Feledziak, J. Marchand-brynaert, V. Stevens, W. Herrebout, C. V Stevens, *Phys Chem Chem Phys* **2012**, 8562–8571.

[24] V. P. Nicu, E. J. Baerends, *Phys Chem Chem Phys* **2009**, *11*, 6107–6118.

[25] V. P. Nicu, E. Debie, W. Herrebout, B. Van der Veken, P. Bultinck, E. J. Baerends, *Chirality* **2009**, *21 Suppl 1*, E287–E297.

[26] S. Góbi, G. Magyarfalvi, *Phys Chem Chem Phys* **2011**, *13*, 16130–16133.

[27] J. Sadlej, J. C. Dobrowolski, J. E. Rode, M. H. Jamróz, *Phys Chem Chem Phys* **2006**, *8*, 101–113.

[28] C. L. Covington, P. L. Polavarapu, *J Phys Chem A* **2013**, *117*, 3377–3386.

[29] J. M. Batista, A. N. L. Batista, D. Rinaldo, W. Vilegas, Q. B. Cass, V. S. Bolzani, M. J. Kato, S. N. López, M. Furlan, L. a. Nafie, *Tetrahedron: Asymmetry* **2010**, *21*, 2402–2407.

[30] F. Wang, P. L. Polavarapu, **2001**, 6991–6997.

[31] S. Shin, M. Nakata, Y. Hamada, *J Phys Chem A* **2006**, *110*, 2122–2129.

[32] G. Longhi, S. Abbate, P. Scafato, C. Rosini, *Phys Chem Chem Phys* **2010**, *12*, 4725–4732.

[33] J. M. Batista, A. N. L. Batista, J. S. Mota, Q. B. Cass, M. J. Kato, V. S. Bolzani, T. B. Freedman, S. N. López, M. Furlan, L. a Nafie, *J Org Chem* **2011**, *76*, 2603–2612.

[34] M. Losada, H. Tran, Y. Xu, *J Chem Phys* **2008**, *128*, 014508.

[35] J. Sadlej, C. Dobrowolski, J. E. Rode, V. Buch, U. Buck, *Chem Soc Rev* **2010**, *39*, 1478–1488.

[36] C. Merten, M. Amkreutz, A. Hartwig, *Phys Chem Chem Phys* **2010**, *12*, 11635–11641.

[37] T. Taniguchi, K. Monde, *J Am Chem Soc* **2012**, *134*, 3695–3698.

[38] T. Wu, X. You, *J Phys Chem A* **2012**, *116*, 8959−8964.

[39] P. L. Polavarapu, A. Petrovic, F. Wang, *Chirality* **2003**, *15 Suppl*, S143–S149.

[40] A. G. Petrovic, A. Navarro-Vázquez, J. L. Alonso-Gómez, *Curr Org Chem* **2010**, 1612–1628.

[41] A. Kraszewska, P. Rivera-Fuentes, G. Rapenne, J. Crassous, A. G. Petrovic, J. L. Alonso-Gómez, E. Huerta, F. Diederich, C. Thilgen, *Eur J Org Chem* **2010**, 4402–4411.

[42] B. Buschhaus, V. Convertino, P. Rivera-fuentes, J. L. Alonso-Gómez, A. G. Petrovic, F. Diederich, *Eur J Org Chem* **2010**, 2452–2456.